

# Adaptive digital linearization of RF power amplifiers

## Linéarisation adaptative numérique d'amplificateurs de puissance RF

Anit Lohtia, Paul A. Goud and Colin G. Englefield,

TR Labs and Department of Electrical Engineering, University of Alberta, Edmonton, Alta. T6G 2G7

The performance of an adaptive digital technique for the linearization of RF power amplifiers is investigated. Cubic spline interpolation is used to estimate the amplifier's AM-AM and AM-PM characteristics. Using the computed characteristic coefficients, the baseband input signal is appropriately predistorted to compensate for the amplifier nonlinearity. This method has significantly better suppression of the intermodulation products than other predistortion techniques. The out-of-band power emission is also significantly reduced. The performance of baseband predistortion linearization techniques is adversely affected by modulator and demodulator impairments. A digital correction technique is presented to compensate for these imperfections. In this technique, part of the RF signal is fed to an envelope detector. The detector output and the baseband signal are used to estimate the impairment values, using the Newton-Raphson method. The estimated impairment values are then used to compensate for the modulator/demodulator impairments. Spurious signals can be suppressed by more than 30 dB using this technique.

Cet article traite de la performance d'une technique adaptative numérique pour la linéarisation d'amplificateurs de puissance RF. Une interpolation spline cubique est utilisée pour estimer les caractéristiques AM-AM et AM-PM de l'amplificateur. À partir des coefficients calculés, le signal d'entrée en bande de base est prédistoronné en vue de compenser la non-linéarité de l'amplificateur. Cette méthode résulte en une suppression significativement meilleure des produits d'intermodulation que d'autres techniques de prédistorion, et la puissance émise hors bande est également réduite de manière significative. La performance des techniques de linéarisation par prédistorion en bande de base est affectée par les imperfections du modulateur et du démodulateur, et une technique de correction numérique est présentée pour leur compensation, dans laquelle une partie du signal RF est envoyée à un détecteur d'enveloppe. La sortie du détecteur et le signal en bande de base sont utilisés pour estimer la valeur des imperfections avec la méthode Newton-Raphson, et pour compenser les imperfections du modulateur/démodulateur. Le niveau des signaux non-désirés peut être réduit de plus de 30 dB.

### I. Introduction

Analogue wireless cellular telephone systems, specifically, AMPS (Advanced Mobile Phone Service), NMT (Nordic Mobile Telephone) and TACS (Total Access Communication System), all use frequency modulation. Since a frequency-modulated signal has a constant envelope, a power-efficient RF amplifier can be used to amplify the signal without generating intermodulation distortion products. However, frequency modulation is not spectrally efficient. Linear modulation techniques are spectrally more efficient than frequency modulation. The North American interim standard (IS-54) specifies  $\pi/4$ -shifted differentially encoded quadrature phase-shift keying ( $\pi/4$ -DQPSK) as the modulation method for digital cellular systems [1]. While  $\pi/4$ -DQPSK modulation is spectrally efficient, it also gives rise to an RF signal that has a fluctuating envelope. Nonlinear amplification of such a modulated signal leads to intermodulation distortion products and spectral spreading. Therefore, to keep the out-of-band power emission below the limits specified by the IS-54 standard, a highly linear RF power amplifier is required to amplify a  $\pi/4$ -DQPSK modulated signal.

A simple way to achieve linear amplification is to back off the amplifier, so that it operates in the linear region of its transfer characteristic. However, using an amplifier in this way provides a low dc-to-RF conversion efficiency. A main challenge in RF power amplifier design is to maintain linearity without compromising the power efficiency of the amplifier.

A number of techniques for the linearization of RF power amplifiers have been reported in the literature. These techniques normally fall into one of the following categories: 1) feedforward, 2) linear amplification using nonlinear components (LINC), 3) negative feedback, and 4) predistortion. Feedforward correction [2] has an open-loop configuration; hence, it is unconditionally stable and is inherently capable of

wide-band signal amplification. However, this technique cannot adapt to drifts in the amplifier characteristic which may occur due to temperature variation, change in power supply voltage, frequency change, etc. The LINC method [3]-[4] uses two well-matched amplifiers. The input signal is split into two constant-amplitude phase-modulated signals which are then amplified separately using two nonlinear RF amplifiers. These signals are then passively summed in such a way that their undesired components are in anti-phase, so that they cancel. LINC requires two well-matched amplifiers, which may not be easy to obtain. Also, this method cannot adapt to drifts in the amplifier characteristics. A modification of the LINC technique, the Combined Analogue Locked Loop Universal Modulator (CALLUM) [5], uses feedback from the output to compensate for drifts in the characteristics of the amplifiers. Cartesian coordinate negative feedback linearization [6]-[7] uses synchronously demodulated signals as the feedback information. These signals are subtracted from the baseband input signals to generate loop error signals. If the loop gain is sufficiently high, the feedback loop will continuously correct for the nonlinearity. This technique is comparatively simple to implement, but the resulting linearity and bandwidth are critically dependent on the loop time delay. Predistortion techniques [8]-[11] operate on the basis of providing an appropriately distorted signal to the amplifier, so that the amplifier output is simply a scaled replica of the original input signal. Some predistortion techniques use fixed signal predistortion circuits prior to amplification. Such circuits cannot compensate for drifts in the amplifier nonlinearities. Several transmitter-based recursive algorithms have been developed to adapt to drifts in the amplifier characteristics. Cavers [10] proposed a complex gain predistorter that takes advantage of the amplitude dependence of the amplifier distortion. This technique uses the secant method to obtain and update the predistortion coefficients. This algorithm, however, is sensitive to the initial conditions, which can prevent convergence [11].

This paper presents a new adaptive predistortion technique for RF power amplifier linearization. The AM-AM and AM-PM characteristics of the amplifier are estimated using cubic spline interpolation, from a look-up table of distortion values that are obtained directly from the amplifier itself using synchronous demodulation. These estimated characteristics are then used to predistort the input signal. In this paper, the performance of this technique is compared with that of the cartesian coordinate negative feedback and complex gain predistortion techniques, using intermodulation products and out-of-band power emission as the key criteria.

A quadrature modulator is required to generate the modulated RF signal for transmission. As well, a quadrature demodulator recovers the baseband feedback signal from the output RF signal. Analogue quadrature modulators and demodulators have three major impairments; namely, gain imbalance, phase imbalance and dc offset. These impairments generate spurious signals that will degrade the performance of a baseband feedback linearization method. This paper also presents a technique for compensating these quadrature modulator and demodulator impairments. For representative modulator/demodulator impairment values, the overall improvement of amplifier linearity is also presented.

**II. Proposed RF power amplifier linearizer**

A block diagram of a transmitter with the proposed linearizer is shown in Fig. 1. The signal source bits, generated as a pseudorandom sequence of length  $2^{31} - 1$ , are encoded, in pairs, into the in-phase ( $i_k$ ) and quadrature ( $q_k$ ) components of the transmitted symbols. An over sampling rate of 16 samples/symbol was used. The  $i_k$  and  $q_k$  components pass through a pulse-shaping filter. The square of the magnitude of the resulting complex signal,  $|v_k|^2$ , is a pointer to a look-up table that contains predistortion coefficients for the  $i$  and  $q$  channels. The signal ( $i_k, q_k$ ) is a vector multiplied by the appropriate complex predistortion coefficient to generate the predistorted signal ( $i_p, q_p$ ), which in turn is converted to two analogue signals by a pair of D/A converters. These analogue signals drive a quadrature modulator that generates the RF signal. The input to the amplifier can be written as

$$x(t) = (i_p^2 + q_p^2)^{1/2} \cos(\omega_c t - \phi_p), \tag{1}$$

where  $\phi_p = \tan^{-1}[q_p/i_p]$ , and  $\omega_c$  is the carrier frequency. A portion of the amplifier output is synchronously demodulated to generate a pair of baseband signals, which are converted to digital signals,  $i_d$  and  $q_d$ , using A/D converters. The quadrature demodulator outputs,  $i_d$  and  $q_d$ , are compared with the inputs to the quadrature modulator,  $i_p$  and  $q_p$ . To estimate the AM-AM and AM-PM characteristics, let

$$v_p = [i_p^2 + q_p^2]^{1/2},$$

$$v_d = [i_d^2 + q_d^2]^{1/2},$$

$$\phi_d = \tan^{-1}[q_d/i_d],$$

$$\Phi = \phi_d - \phi_p, \text{ the phase distortion introduced by the amplifier.}$$

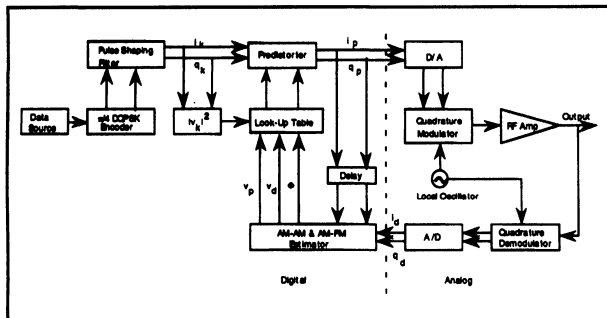


Figure 1: Block diagram of a  $m$ -QPSK transmitter with the proposed linearizer.

For a small number of values of  $v_p$ , corresponding values of  $v_d$  and  $\Phi$  are stored in memory. These values of  $v_p$  are sampled in predetermined intervals. From trial simulations, it was found that 30 different values of  $v_p$  were sufficient to accurately define the amplifier's amplitude and phase characteristic. Note that the points do not need to be equally spaced; they must, however, be spread over the entire range of the input signal. Since there is delay in the feedback path, the input signal must be delayed by the same amount. Methods of measuring and implementing this delay are discussed in [8] and [11]. Using these stored values, cubic spline interpolation [12] is used to estimate the AM-AM and AM-PM characteristics for any particular  $|v_k|^2$  value. For equivalent accuracy using a single polynomial fit, a high-order polynomial would be required. Predistortion coefficients are computed using the estimated AM-AM and AM-PM characteristics. For a given input power level,  $x_m$ , the desired output power level,  $y_c$ , is known from the required linear characteristic, as shown in Fig. 2. If the input signal,  $x_m$ , is fed to the amplifier without predistortion, the output power would be  $y_a$ , which does not lie on the linear characteristic. To obtain the desired output power,  $y_c$ , the input to the amplifier should be  $x_p$ . The inverse AM-AM characteristic is directly computed from the measured distortion values. For the corrected value of magnitude,  $x_p$ , the corresponding value of phase distortion ( $\Phi$ ) can be read from the estimated AM-PM characteristic.

The proposed linearizer makes use of the fact that the amplitude and phase distortion of a narrow-band RF power amplifier are dependent only upon the amplitude of the input signal and are independent of the phase of the input signal [10]. In other words, input signals with equal magnitude suffer identical amplitude and phase distortion. However, analogue quadrature modulator and demodulator impairments can introduce phase-dependent distortion into the system and can degrade the performance of the linearizer.

**III. Quadrature modulator and demodulator impairments**

Fig. 3 shows a schematic diagram of a typical quadrature modulator. The modulator consists of four components; namely, two mixers, a quadrature hybrid and an in-phase power combiner. These components are not ideal, resulting in a collective effect that can be represented by gain imbalance, phase imbalance and dc offset [13]-[16]. Gain imbalance represents the gain mismatch between the  $i$  and  $q$  channels. Ideally, the gains in the  $i$  and  $q$  channels are equal. If the phase difference between the local oscillator signals for the  $i$  and  $q$  channels is not exactly  $90^\circ$ , phase imbalance exists. A difference in the lengths of the two RF paths can result in a frequency-dependent phase imbalance. Lastly, carrier feedthrough gives an unwanted RF component at the carrier frequency. The quadrature demodulator suffers from similar impairments. The gain and phase errors result in image signals

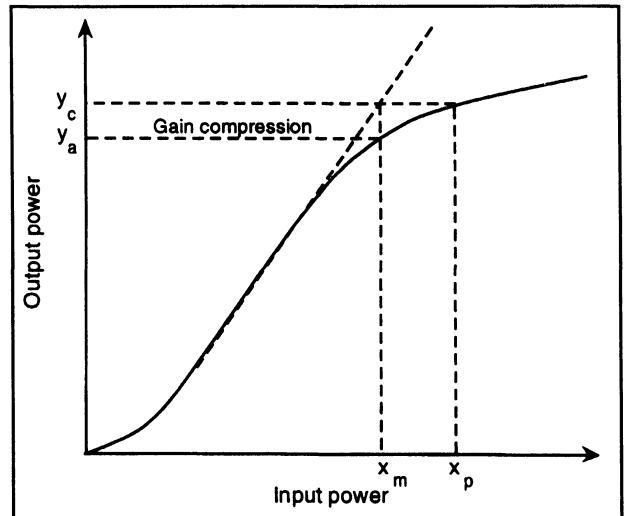


Figure 2: Power transfer characteristic of an amplifier.

that are independent of dc offset. The image signals due to the gain and phase error are 90° out of phase. Self-mixing of the carrier in the mixer can cause dc offset.

For a single-tone input signal to the modulator with frequency  $f_m$ , gain and phase imbalance will generate a spurious tone at frequency  $f_m$  below the carrier frequency. The dc offset generates a spurious signal at the carrier frequency. These spurious signals can add to the intermodulation distortion products when the composite signal is passed through the amplifier nonlinearity. Therefore, spurious signals must be kept at the minimum level possible. Gain imbalance distorts a circular modulation constellation into an elliptical constellation. Phase imbalance causes rotation of the axes of this ellipse. The dc offset shifts all constellation points by an equal amount.

**A. Quadrature modulator and demodulator impairment compensators**

The output of an ideal quadrature modulator can be written as

$$s(t) = i(t) \cos \omega_c t + q(t) \sin \omega_c t, \tag{2}$$

where  $i(t)$  and  $q(t)$  are the in-phase and quadrature-phase components respectively. However, a practical quadrature modulator has gain imbalance, phase imbalance and dc offset. Therefore, the output of a practical quadrature modulator would be given by

$$s(t) = [a_1 i(t) + b_1] \cos(\omega_c t + \phi) + [a_2 q(t) + b_2] \sin \omega_c t, \tag{3}$$

where  $a_1, a_2$  are gains, and  $b_1, b_2$  are dc offsets for the  $i$  and  $q$  channels respectively, and  $\phi$  is the phase imbalance between the  $i$  and  $q$  channels.

Equation (3) can be simplified to

$$s(t) = m(t) \cos[\omega_c t + \theta(t)], \tag{4}$$

where

$$m(t) = \left\{ [(a_1 i(t) + b_1) \cos \phi]^2 + [(a_1 i(t) + b_1) \sin(-\phi) + (a_2 q(t) + b_2)]^2 \right\}^{1/2} \tag{5}$$

and

$$\theta(t) = \tan^{-1} \left[ \frac{(a_1 i(t) + b_1) \sin(-\phi) + (a_2 q(t) + b_2)}{(a_1 i(t) + b_1) \cos \phi} \right]. \tag{6}$$

A block diagram of the proposed compensator for the modulator impairments is shown in Fig. 4. A portion of the modulator output is fed to an envelope detector. The digitized detector output,  $m$ , and the corresponding values of the quadrature inputs ( $i_d, q_d$ ) to the modulator

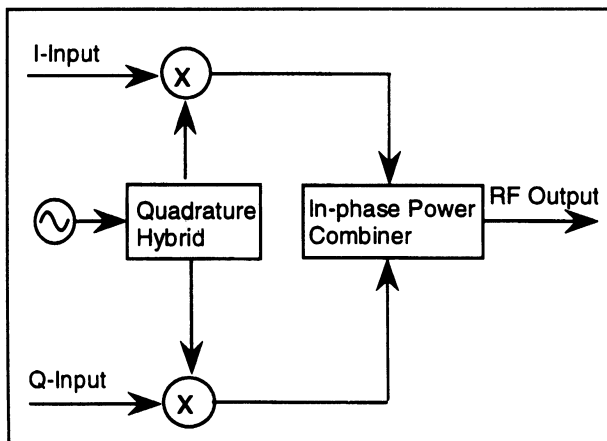


Figure 3: Schematic diagram of an analogue quadrature modulator.

are stored in memory. There are five unknowns in (5); namely,  $a_1, a_2, b_1, b_2$ , and  $\phi$ . Therefore, five independent equations are needed to solve for these unknowns. Five sets of values of  $m, i_d$  and  $q_d$ , obtained at five different time instants, are used to generate five independent equations that are solved using the multivariate Newton-Raphson method [12]. In the actual computations,  $m^2$  is used in order to avoid taking the square root. To generate independent equations and ensure convergence of the Newton-Raphson method, the values of  $m, i_d$  and  $q_d$  should be well spread out over the signal constellation. The initial values for the Newton-Raphson iterations are taken to be no gain imbalance, no dc offset, and no phase imbalance (i.e., the ideal values  $a_1 = a_2 = 1, b_1 = b_2 = 0, \phi = 0$ ). With these initial conditions, the Newton-Raphson iterations always converged for reasonable impairment values. With the impairment values known, the  $i$  and  $q$  signals are predistorted to correct for the modulator imperfections. To update the estimated values of the impairments, a new set of values of  $m, i_d$  and  $q_d$  is measured and stored in memory, and the impairment values estimated as before.

The structure of the demodulator impairment compensator is similar to that of the modulator impairment compensator, as shown in Fig. 5. The input to the envelope detector is a portion of the RF signal,  $s(t)$ . If  $s(t)$  is given by (2), then the outputs of an ideal quadrature demodulator would be  $i$  and  $q$ . However, the outputs of a practical quadrature demodulator will be

$$i'(t) = a_3 [i(t) \cos \phi + q(t) \sin(-\phi)] + b_3, \tag{7}$$

$$q'(t) = a_4 q(t) + b_4. \tag{8}$$

The envelope detector output is given by

$$m = \left[ \left( \frac{1}{\cos \phi} \left( \frac{i' - b_3}{a_3} + \frac{q' - b_4}{a_4} \sin \phi \right) \right)^2 + \left( \frac{q' - b_4}{a_4} \right)^2 \right]^{1/2}. \tag{9}$$

The digitized detector output,  $m$ , along with the corresponding demodulated values  $i'$  and  $q'$ , are stored in memory. As in the case of the

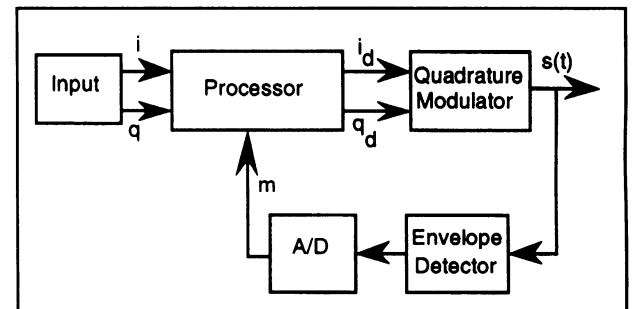


Figure 4: Quadrature modulator impairment compensator.

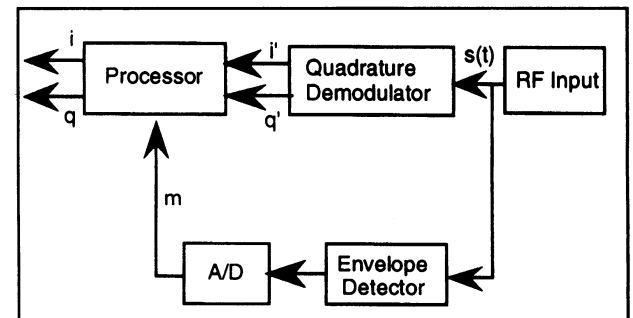


Figure 5: Quadrature demodulator impairment compensator.

modulator, there are five unknowns in (9); namely:  $a_3, a_4, b_3, b_4$  and  $\phi$ . Therefore, five independent equations are needed to solve for these unknowns. Five sets of values of  $m, i'$  and  $q'$ , obtained at five different time instants, are used to generate five independent equations that are then solved using the Newton-Raphson method. As previously,  $m^2$  is used in (9). The estimated impairment values are used to post-distort  $i'$  and  $q'$  in order to correct for the demodulator impairments.

IV. Simulation models

A complex envelope simulation model has been used to compare the performance of the different linearization techniques. Band-pass signals are represented by equivalent low-band signals. Simulation models include a random data source, a  $\pi/4$ -DQPSK modulator and a square-root raised cosine pulse-shaping filter ( $\pi = 0.35$ ). The parameters used for the amplifier models were obtained from actual measurements of the AM-AM and AM-PM characteristics of nonlinear

power amplifiers that were tested in the laboratory. The characteristics for the class AB and class B amplifiers are shown in Figs. 6 and 7 respectively. The class AB amplifier is an Avantek 6-W amplifier specially designed for the North American cellular frequency band. The class B amplifier uses a Philips BLV93 transistor, with a nominal maximum output power of 8 W.

The performance of different linearization techniques has been evaluated using the power spectral density (PSD) and intermodulation distortion product power levels as the performance criteria. The output data are windowed by a Blackman window to reduce the spectral leakage. Overlapping sets of data are averaged together to reduce the variance in each frequency sample. The intermodulation distortion products have been evaluated using a two-tone input signal. The test signal has two complex tones, one at 20 kHz and one at 25 kHz, a cosine wave being used for the  $i$  component, and a sine wave for the  $q$  component.

V. Results

A comparison of the performance of the proposed linearization technique with cartesian coordinate negative feedback and complex gain predistortion linearization is shown in Fig. 8. For the cartesian coordinate negative feedback technique, a loop gain of 25 dB and

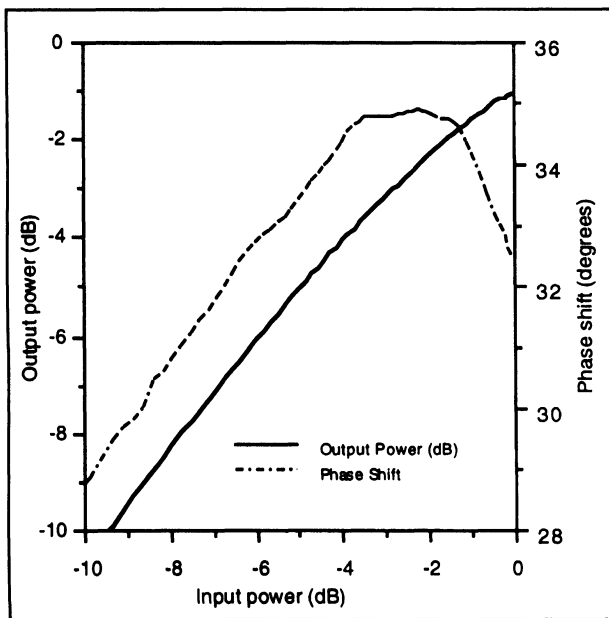


Figure 6: Transfer characteristics of the experimental class AB amplifier.

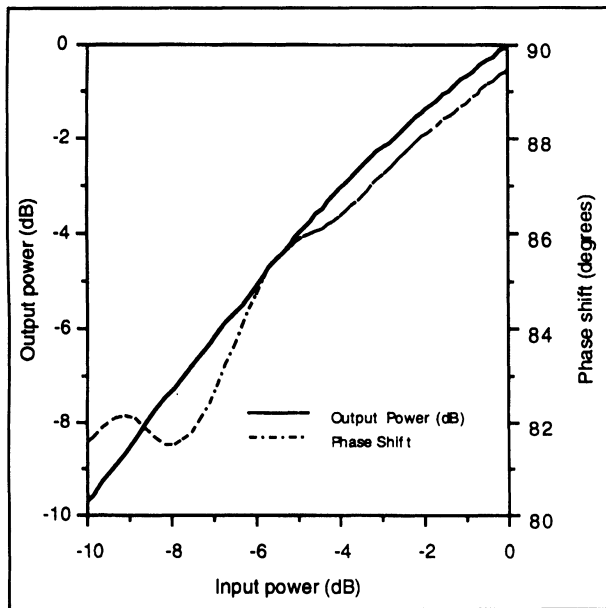
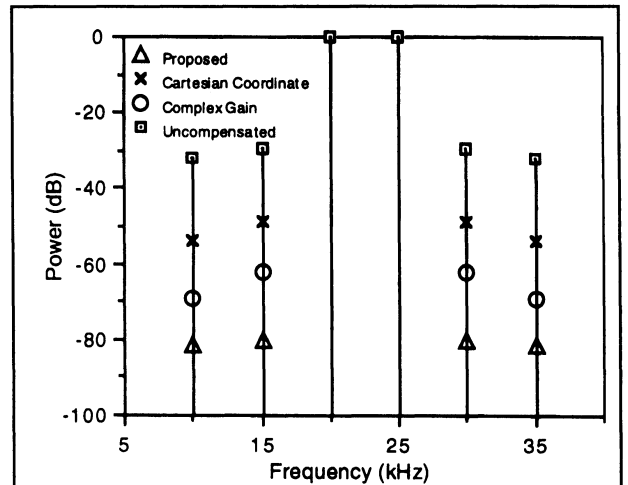
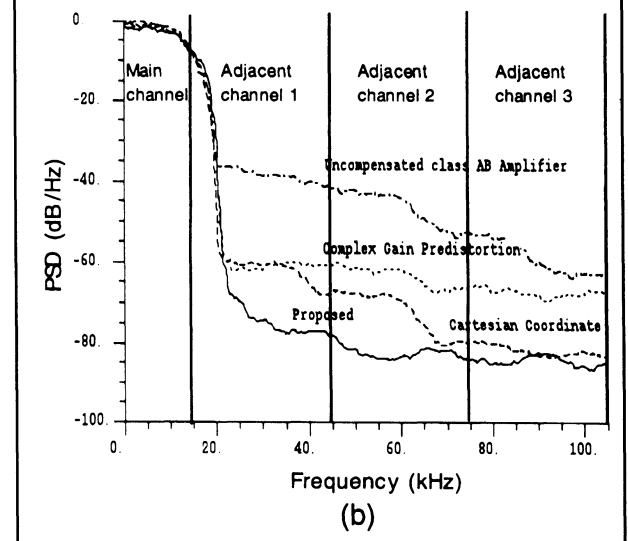


Figure 7: Transfer characteristics of the experimental class B amplifier.



(a)



(b)

Figure 8: Linearized class AB amplifier performance: (a) intermodulation products  $IM_3$  at 15 and 30 kHz and  $IM_5$  at 10 and 15 kHz; (b) power spectral density.

bandwidth of 100 kHz were used. For the complex gain predistortion technique, 64 points were used. For the cubic spline interpolation technique, 30 spline points were used. In all the tests, the peak RF amplifier power was set at the 1-dB gain compression point. This point corresponds to the 0-dB input level in Figs. 6 and 7. The third-order ( $IM_3$ ) and fifth-order ( $IM_5$ ) intermodulation distortion products for the uncompensated class AB amplifier were found to be  $-29.6$  dB and  $-31.8$  dB respectively. The proposed technique reduces  $IM_3$  and  $IM_5$  to  $-80.3$  dB and  $-81.2$  dB respectively. The better performance observed in the cubic spline interpolation is due to better curve fitting of the AM-AM characteristic than the complex gain predistortion that uses a linear interpolation technique. The  $IM_3$  and  $IM_5$  are  $-62$  dB and  $-69$  dB respectively when complex gain predistortion is used. The cartesian coordinate negative feedback reduces  $IM_3$  and  $IM_5$  to  $-49$  dB and  $-54$  dB respectively. Fig. 8(b) shows the output power spectral density for the three linearization methods. The proposed technique is seen to have significantly better performance than cartesian coordinate negative feedback in the first and second adjacent channels, and similar performance in the third adjacent channel. A comparison of results for the class B amplifier is shown in Fig. 9.

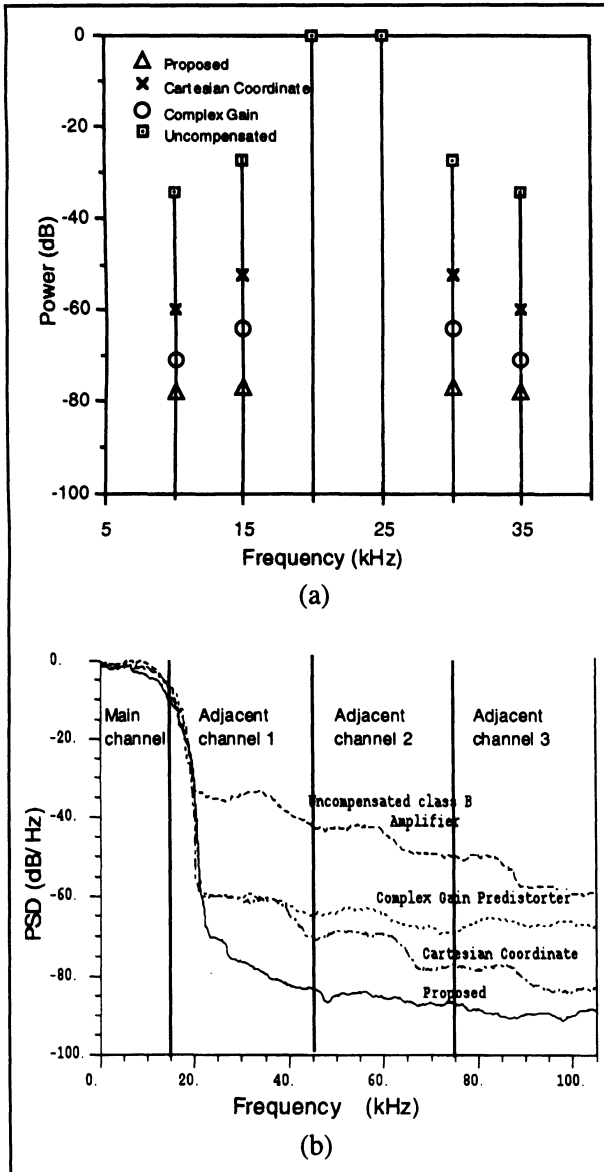


Figure 9: Linearized class B amplifier performance: (a) intermodulation products  $IM_3$  at 15 and 30 kHz and  $IM_5$  at 10 and 15 kHz; (b) power spectral density.

Fig. 10 shows the level of the undesired sideband in a quadrature modulator with and without an impairment compensator. The input test signal is a 20-kHz complex tone. The sideband level is shown as a function of gain imbalance, with phase imbalance as a parameter. The undesired sideband is seen to be about 70 dB below the desired sideband level when the compensator is used. There is a variation of about 25 dB in the suppressed sideband. This variation is attributable to the convergence characteristics of the iterative process in the Newton-Raphson method. The convergence is not monotonic, and depends on the starting value. As a result, the undesired sideband level for a higher gain and/or phase imbalance can actually be less than that for a smaller imbalance. It should be noted, however, that convergence is always obtained for small impairment values, and that decreasing the convergence bound leads to improved performance. This is demonstrated in Fig. 11, which shows the undesired sideband level of a modulator compensator as a function of the convergence bound for Newton-Raphson iterations. It is seen that decreasing the convergence bound increases the suppression of the undesired sideband. Decreasing the convergence bound, however, requires more iterations of the convergence algorithm. With a convergence factor of  $10^{-3}$ , the number of iterations is normally less than 20. (A convergence factor of  $10^{-3}$  implies that the iteration is stopped when the fractional change of each parameter during one iteration is less than this value. Each iteration is one pass through all five equations.) The compensator works well for up to about 12% gain imbalance,  $12^\circ$  phase imbalance and 12% dc offset. For greater values of the impairments, the Newton-Raphson iterations do not converge. The failure of the compensator correction algorithm is thus sudden, rather than a smooth deterioration.

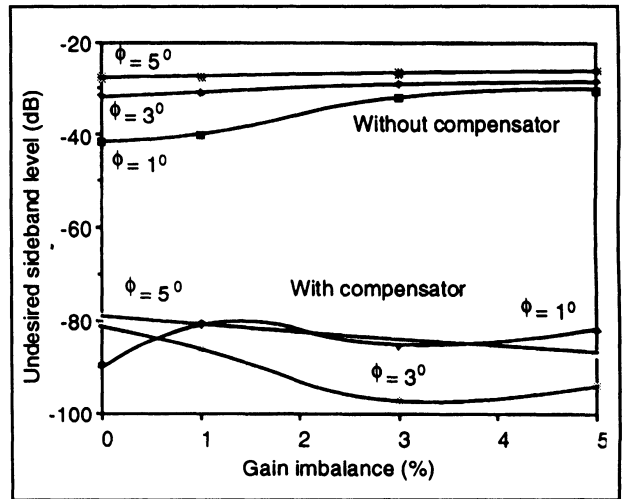


Figure 10: Undesired sideband level versus gain imbalance.

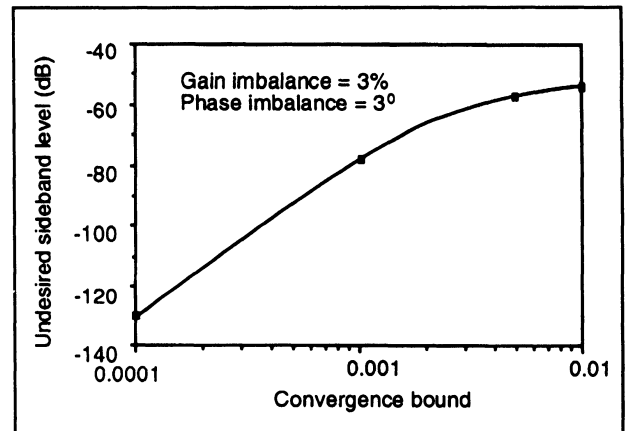


Figure 11: Undesired sideband level versus convergence bound of modulator compensator.

Similar results are obtained for the quadrature demodulator impairment compensator; these are shown in Figs. 12 and 13.

**VI. Discussion**

The proposed linearizer is suitable for baseband implementation. Since it is basically an open-loop configuration, it is unconditionally stable. The feedback loop is closed only during updating of the predistortion coefficients. This linearization method is not restricted by the modulation format, because the signal is predistorted after the pulse-shaping filter. Although the AM-AM and AM-PM characteristics of the class AB and class B amplifiers are significantly different (see Figs. 6 and 7), the linearizer performs almost equally well for both amplifiers.

The linearizer assumes the distortion to be dependent only on the magnitude of the input signal. However, phase-dependent distortion can occur due to the quadrature modulator and demodulator impairments. The performance of the proposed linearizer is critically dependent on the quadrature modulator and demodulator performance. The quadrature modulator and demodulator impairments need to be compensated for to ensure satisfactory performance of the amplifier linearizer. The overall linearized system with the quadrature modulator and demodulator impairment compensator will be a multiple-loop system. The effect of modulator and demodulator impairments on the performance of the linearized amplifier is illustrated in Fig. 14. For both the modulator and demodulator the impairments are taken to be 3% gain imbalance, 3° phase imbalance, and 3% dc offset. These values are fairly typical for practical modems. It is seen from the figure

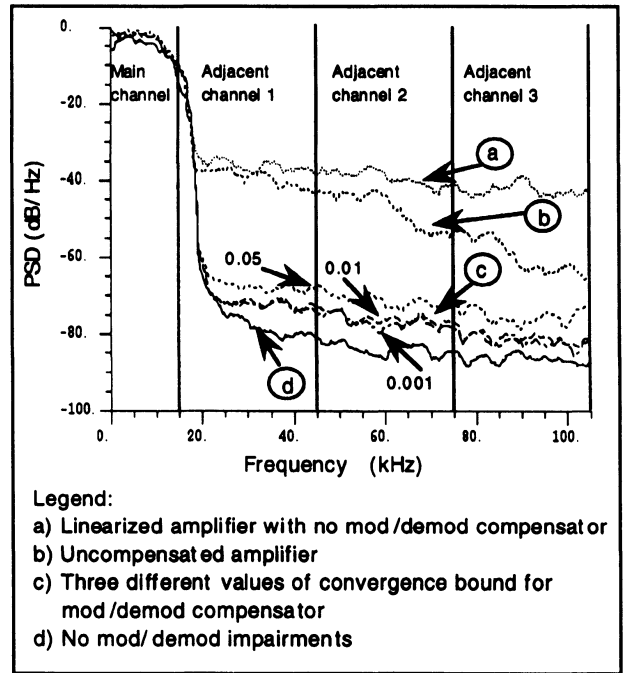


**Figure 14:** Overall system performance for three different values of convergence bound for the modulator and demodulator impairment compensator.

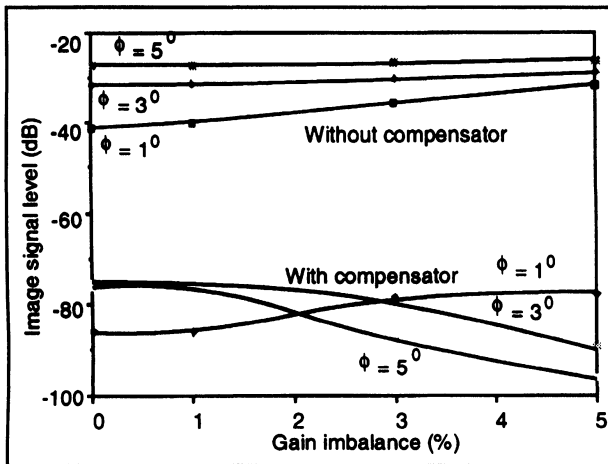


**Figure 12:** Image signal level versus gain imbalance.

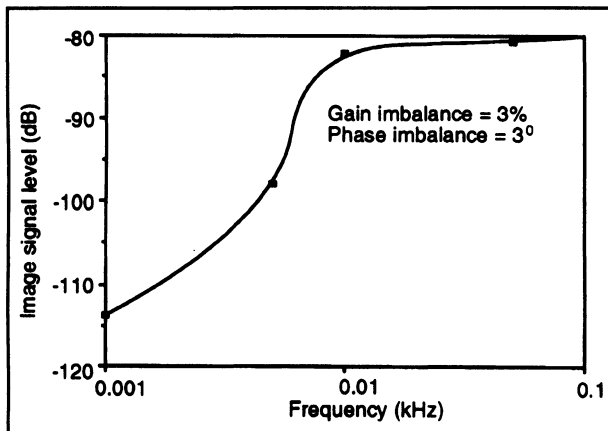


**Figure 13:** Image signal level versus convergence bound of demodulator impairment compensator.

that, if no compensation is used to correct for these errors, then the overall performance of the linearizer is actually worse than if the amplifier is unlinearized. A modest degree of modulator and demodulator compensation results in a significant improvement in the performance of the linearized amplifier. If the convergence bound for the modulator and demodulator compensation is set at 0.05, then the out-of-band power for the overall amplifier drops by about 30 dB; for convergence bounds of 0.01 and 0.001, there are further improvements of 6 dB.

These simulations did not investigate the effects of noise on the performance of the technique. However, since all the circuitry is within the transmitter, the only significant sources of noise are the A/D and D/A converters. Envelope detector inaccuracy will affect the modulator and demodulator impairment compensator performance.

**VII. Conclusion**

An improved adaptive technique for the linearization of RF power amplifiers with narrowband signals has been evaluated. The linearizer can compensate for slow drifts of the amplifier characteristics. The IM<sub>3</sub> and IM<sub>5</sub> can be suppressed about 80 dB below the tone levels using this linearization method. The technique has been used to linearize both class AB and class B amplifiers.

An adaptive technique for the compensation of quadrature modulator and demodulator impairments has also been studied. The technique works well for up to about 12% gain imbalance, 12° phase imbalance and 12% dc offset. The spurious signals generated by the quadrature modulator can be suppressed by more than 30 dB using the modulator impairment compensation technique.

**Acknowledgements**

The authors thank NovAtel Communications Ltd., especially Dr. Andrew Wright, for providing the amplifier distortion measurements, and for helpful discussions. The assistance of Mr. Timothy Neufeld with computer simulations is also acknowledged.

## References

- [1] EIA/TIA Interim Standard, *Cellular System Dual-Mode Mobile Station – Base Station Compatibility Standard, IS-54*, Electronic Industries Association, Washington, D.C., May 1990.
- [2] R.D. Stewart and F.F. Tusubira, "Feedforward linearization of 950 MHz amplifiers," *IEEE Proc.*, vol. 135, pt. H, no. 5, Oct. 1988, pp. 347-350.
- [3] D.C. Cox, "Linear amplification with nonlinear components," *IEEE Trans. Comm.*, vol. COM-22, no. 12, Dec. 1974, pp. 1942-1945.
- [4] F.H. Raab, "Efficiency of outphasing RF power-amplifier systems," *IEEE Trans. Comm.*, vol. COM-33, no. 10, Oct. 1985, pp. 1094-1099.
- [5] A. Bateman, "The combined analogue locked loop universal modulator (CALLUM)," in *Proc. 42nd IEEE Veh. Techn. Conf.*, Denver, Colo., May 1992, pp. 759-763.
- [6] A. Bateman, R.J. Wilkinson and J.D. Marvill, "The application of digital signal processing to transmitter linearisation," in *Proc. 8th European Conf. Electrotech.*, Stockholm, Sweden, June 1988, pp. 64-67.
- [7] M. Johansson and T. Mattsson, "Transmitter linearization using cartesian coordinate negative feedback for linear TDMA modulation," in *Proc. 41st IEEE Veh. Techn. Conf.*, St. Louis, Mo., May 1991, pp. 439-444.
- [8] Y. Nagata, "Linear amplification technique for digital mobile communications," in *Proc. 39th IEEE Veh. Techn. Conf.*, San Francisco, Calif., May 1989, pp. 159-164.
- [9] A.A.M. Saleh and J. Salz, "Adaptive linearization of power amplifier in digital radio systems," *Bell Syst. Tech. J.*, vol. 62, no. 4, Apr. 1983, pp. 1019-1033.
- [10] J.K. Cavers, "Amplifier linearization using a digital predistorter with fast adaptation and low memory requirements," *IEEE Trans. Veh. Techn.*, vol. VT-39, no. 4, Nov. 1990, pp. 374-382.
- [11] A.S. Wright and W.G. Durtler, "Experimental performance of an adaptive digital linearized power amplifier," *IEEE Trans. Veh. Techn.*, vol. VT-41, no. 4, Nov. 1992, pp. 395-400.
- [12] S. Yakowitz and F. Szidarovszky, *An Introduction to Numerical Computations*, New York: Macmillan Publishing Company, 1989.
- [13] D.E. Norton, S.A. Massa and P. O'Donovan, "I and Q modulators for cellular communications systems," *Microwave J.*, vol. 34, no. 10, Oct. 1991, pp. 63-80.
- [14] J. Roome, "Analysis of quadrature detectors using complex envelope notation," in *IEEE Proc.*, vol. 136, pt. F, no. 2, Apr. 1989, pp. 95-100.
- [15] J.K. Cavers and M. Liao, "Adaptive compensation for imbalance and offset losses in direct conversion transceivers," in *Proc. 41st IEEE Veh. Techn. Conf.*, St. Louis, Mo., May 1991, pp. 578-583.
- [16] M. Faulkner, T. Mattsson and W. Yates, "Automatic adjustment of quadrature modulators," *Electron. Lett.*, vol. 127, no. 3, Jan. 1991, pp. 214-216.